Canadian Mineralogist
Vol. 23, pp. 369-379 (1985)

THE HYDROTHERMAL CONVERSION OF HORNBLENDE TO BIOTITE

GEORGE H BRIMHALL, CARL AGEE AND ROGER STOFFREGEN
Department of Geology and Geophysics, University of California, Berkeley, California 94720, U.S.A.

ABSTRACT

Preliminary experiments on the biotitization of primary igneous hornblende have been completed over a temperature range of 300 to 500°C at 1000 bars argon gas pressure. The experiments were run with 0.10 m K_2SO_4–H_2SO_4 aqueous solutions and buffered by a solid assemblage of magnetite, microcline, quartz and pyrite. This buffer fixed oxygen and sulfur fugacities at values appropriate for a felsic intrusive rock undergoing potassic alteration in the early stage of the porphyry-copper environment. In these experiments hornblende was destroyed, producing biotite and anhydrite presumably by the generalized reaction hornblende + K_2SO_4 + H_2SO_4 → biotite + anhydrite + quartz; the Ca^{2+} liberated from the hornblende goes to make anhydrite. Biotitization of hornblende and re-equilibration of primary igneous biotite to lower Fe and Ti and higher Mg contents have been described in high-temperature alteration assemblages around the world (Roberts 1973, Moore & Czamanske 1973, Titley 1982). These reactions, in addition to replacement of titanite by anhydrite and Fe–Ti oxides, may represent the earliest and most widespread effects in granitic wallrocks, as magmatic sulfate-rich hydrothermal solutions begin convective circulation around porphyries. Single-crystal diffraction studies of the products of experiments indicate that the solid–solid transformation of hornblende to biotite occurs with a preferential growth of biotite in crystallographic orientation on the hornblende. Tunnels parallel to the *C* axis of hornblende could be conduits for fast-diffusing ions during alteration.

Keywords: porphyry-copper deposit, hornblende, biotite, acid sulfate fluids, potassium alteration, biotitization of hornblende, diffusion, tunnels.

SOMMAIRE

On a effectué, en expériences préliminaires, la transformation en biotite d'une hornblende primaire entre 300 et 500°C à une pression d'argon de 1000 bars. Les expériences se font en présence d'une solution aqueuse de K_2SO_4–H_2SO_4 (0.10 m) tamponnée par l'assemblage magnétite–microcline–quartz–pyrite. Ce tampon fixe les fugacités d'oxygène et de soufre à des valeurs réalistes pour un pluton felsique sujet à une altération potassique, à un stade précoce d'un environnement de porphyre cuprifère. La hornblende est détruite dans ces expériences, et les produits, biotite + anhydrite, seraient dus à la réaction généralisée hornblende + K_2SO_4 + H_2SO_4 → biotite + anhydrite + quartz, dans laquelle le Ca^{2+}, libéré de la hornblende, forme l'anhydrite. La biotitisation de la hornblende et la ré-équilibration de la biotite primaire en biotite appauvrie en Fe et Ti et enrichie en Mg sont caractéristiques d'assemblages d'altération à haute température (Roberts 1973, Moore & Czamanske 1973, Titley 1982). Ces réactions, ainsi que le remplacement de la titanite par anhydrite + oxydes de Fe–Ti, signaleraient les effets précoces et très répandus sur les parois granitiques des solutions magmatiques riches en sulfate qui circulent par convection près des porphyres. Des études par diffraction X sur cristaux uniques des produits de réaction montrent que la transformation solide–solide de hornblende en biotite mène à une orientation préférentielle de la biotite sur la hornblende. Des tunnels parallèles à l'axe C de la hornblende seraient des conduit pour les ions à diffusion rapide pendant l'altération.

(Traduit par la Rédaction)

Mots-clés: gisement de porphyre cuprifère, hornblende, biotite, fluides acides à sulfate, altération potassique, biotitisation de la hornblende, diffusion, tunnels.

INTRODUCTION

Pervasive biotitic alteration, which entails the partial or complete replacement of specific minerals by biotite in wall rock and in the porphyry host intrusive body, has been described in numerous porphyry-copper deposits (Titley 1982). Biotitization of hornblende, the most common alteration of this type, occurs in broad aureoles extending well beyond the limits of mineralization (Fig. 1). The zone of biotitization is generally symmetrical with respect to zones containing the earliest hydrothermal stages of deposition of copper and molybdenum sulfides, which have a fracture-controlled disseminated occurrence (Roberts 1973). In detail, near the outer fringes of this zone, where islands of unaltered wallrock persist, biotitization of hornblende can be shown to be clearly related to the same veinlets that control alteration halos of the potassic or potassium silicate type; these veinlets contain alkali feldspar, muscovite, andalusite, biotite, quartz and anhydrite (Roberts 1973, Brimhall 1977). Using a variety of geothermometers, a relatively high range of temperatures is indicated for the early hydrothermal systems (570–700°C) (Brimhall 1977, Roberts 1973, Jacobs & Parry 1979). It has been suggested that the biotitization process is related to the initial development of controlling fractures and represents the first hydrothermal stage in a long-lived sequence of fracturing during which convective circulation of fluid occurred (Titley 1982), attended by an evolving composition of the fluid (Brimhall 1977). The close genet-

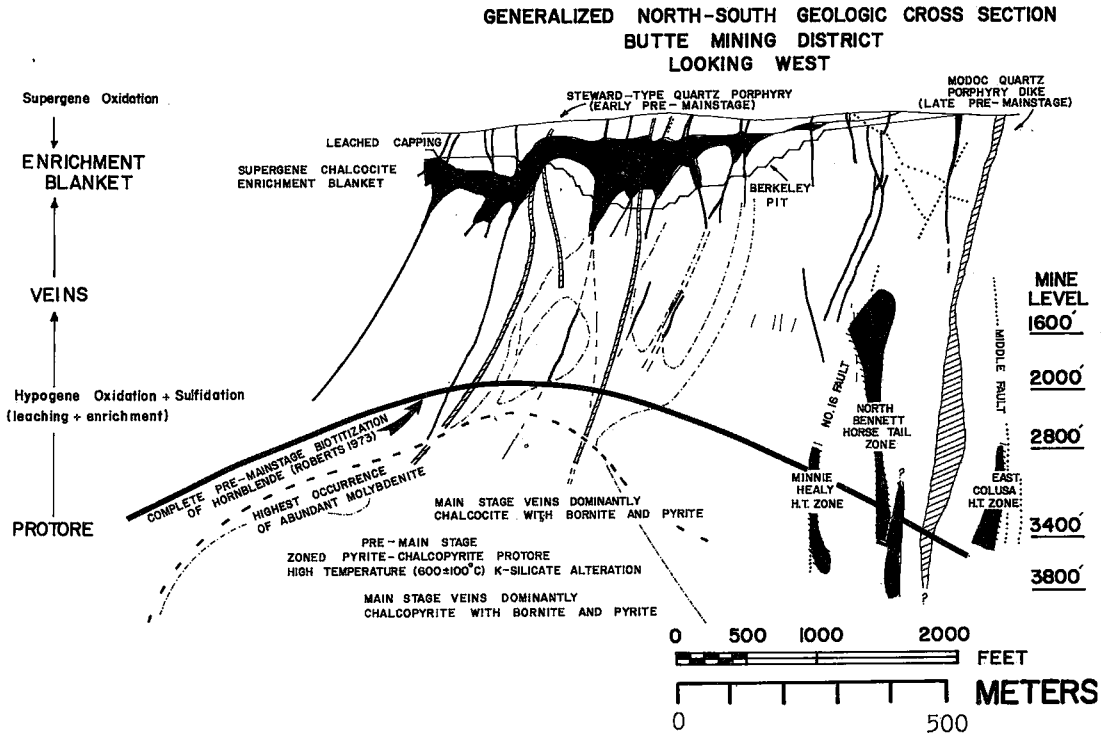

FIG. 1. Generalized vertical cross-section of the Butte District of Montana, showing the subsurface zone of completely biotitized hornblende from the work of Roberts (1973). Its relationship to the various elements in the ore deposit is shown, including supergene chalcocite enrichment blanket, Main Stage Veins, and pre-Main Stage molybdenite and disseminated chalcopyrite–pyrite protore (Brimhall 1979, 1980, Brimhall & Ghiorso 1983, Brimhall *et al.* 1984).

ic association with intrusive phenomena is indicated by the pervasive biotitization observed in magmatic–hydrothermal breccias at the apical portions of porphyry dykes, where hydrofracture density is highest (Brimhall 1977). The first introduction of copper into the wallrocks occurred in this environment in the Butte District of Montana.

Although the space–time pattern, temperature, and magmatic–hydrothermal affinity of biotitization have been well documented, there is a lack of experimental data pertinent to an understanding of (1) the chemical characteristics of the fluids responsible, (2) the reaction chemistry of the hornblende-to-biotite transformation, (3) the crystallographic mechanisms of the solid-state transformation, and (4) its relationship to deposition of chalcopyrite and pyrite, mainly at sites of mafic minerals.

PETROGRAPHY

The Butte District of Montana provides an ideal opportunity to study the effects of biotitization, as the quartz monzonite wallrock is equigranular and homogeneous throughout the district. Petrographic studies have shown that a number of persistent mineralogical effects attend biotitization (Roberts 1973). Igneous hornblende is converted pseudomorphically to a mixture of shreddy hydrothermal biotite, anhydrite and quartz, whereas titanite is replaced by a mixture of ilmenite, hematite, quartz, rutile and anhydrite. Igneous biotite is rimmed by shreddy biotite or alkali feldspar, and generally contains small exsolved grains of rutile. Both the igneous and the shreddy biotite in these rocks are lower in Ti and higher in Mg than biotite from unaltered samples. Pyrite and chalcopyrite occur as minute grains in both biotitized hornblende and igneous biotite.

Using these mineralogical observations, we have designed a number of hydrothermal experiments to understand how the biotitization of hornblende proceeds, what the necessary solutes are in the hydrothermal fluid, what controls the extent of the replacement reaction, and over what time scale the solid transformation proceeds.

EXPERIMENTAL PROCEDURE

Following heavy-liquid separation in acetylene

tetrabromide, a nonmagnetic fraction of fresh hornblende was extracted from a specimen of Butte quartz monzonite. Grains were sorted by dry screening to a mean grain-size of 155 μm. Their habit is prismatic; length and width of the prisms average 201 and 109 μm, respectively. In order to remove fine particles from hornblende surfaces, the sample was washed ultrasonically in distilled water. Additional reactants were selected to act as a buffering assemblage during the experiment; quartz, pyrite, chalcopyrite, rutile and microcline were taken from comparatively pure natural specimens and crushed to a fine grain-size in an agate crucible. Reagent-grade magnetite and anhydrite were used to complete the buffering assemblage, simulating the pre-Main Stage potassium silicate alteration-assemblage (Brimhall 1977, 1979, 1980, Brimhall & Ghiorso 1983).

A 0.10 molar H_2SO_4 and 0.10 molar K_2SO_4 reactant fluid was injected, using a positive displacement micropipette, into 7.5-cm seamless gold tubes containing the experimental charges. The tubes were crimped and welded shut using an oxyacetylene microtorch. The tubes were kept at room temperature by partial submergence in water during welding. Immediately after welding, the capsules were inserted into 0.96-cm-bore 310 alloy stainless steel cold-seal rod bombs fitted with filler rods. Experiments were carried out in horizontal Hoskins electrical furnaces equipped with chromel–alumel thermocouples wired to Wheelco temperature controllers. A continuously recording Honeywell potentiometer monitored the temperature of the experiments. Argon gas was used as the pressure medium and maintained at a confining pressure of 1000 bars.

Following each experiment, quenching was done at pressure by submerging the rod bombs in cold water, and the gold capsule was quenched in cold distilled water for five seconds upon withdrawal from the bomb. The contents of the capsule were removed, and fluid was microfiltered and collected with a digital pipette; solids were immediately washed thoroughly with distilled water and left to dry at room temperature. The time between initial quench and final washing of solids was on the order of two to three minutes.

A quick initial check for the survival of magnetite in the buffering assemblage was done with a hand magnet, after which the solid products were cast in epoxy grain-mounts. A polished thin section was prepared from the hardened casting, such that it could be used for both petrographic examination and electron-microprobe analyses.

Careful inspection of the solid products was performed with a petrographic microscope using both reflected and transmitted light. An inventory of the minerals in the buffer assemblage was made to confirm that the starting quantities had been sufficient to insure a surplus throughout the hydrothermal reaction. Special note was made of the estimated amount of pseudomorphic replacement of hornblende by biotite, and selected grains were chosen for electron-microprobe analysis. All electron-microprobe work was done with an eight-channel Applied Research Laboratories model SEMQ, using biotite standards analyzed by wet-chemical methods.

Experimental Conditions and Textural Results

A total of ten experiments were carried out, at temperatures of 300 to 500°C, with partial to complete biotitization of hornblende observed in all cases. The biotite produced in these reactions, whether rimming or completely replacing the hornblende, is invariably light yellow brown, has the characteristic grainy surface texture of biotite, and appears homogeneous in transmitted light, although compositional heterogeneity on a small scale is apparent in microprobe studies (see below). At relatively low values of the

TABLE 1. DETAILS OF EXPERIMENT DESIGN INCLUDING VOLUMES OF SOLID AND AQUEOUS REACTANTS AND RESULTING TEXTURES—SERIES I-CAGB

	EXPT. 1	EXPT. 2	EXPT. 4
	SOLIDS		
Hornblende	0.0045 cm^3	0.0045 cm^3	0.0124 cm^3
Quartz	0.0058	0.0042	0.0039
Pyrite	0.0052	0.0083	0.0062
Microcline	0.0096	0.0094	0.0093
Magnetite	0.0358	0.0175	0.0190
Anhydrite	0.0048	0.0060	0.0054
	FLUIDS		
0.10 H_2SO_4 – K_2SO_4	1.308 cm^3	1.151 cm^3	0.668 cm^3
PRESSURE	1Kbar	1Kbar	1Kbar
TEMPERATURE	300°C	400°C	500°C
DURATION	21 days	21 days	21 days
RESULTING TEXTURE	Complete biotitization	Complete biotitization	Biotite rims, hornblende cores

TABLE 2. DETAILS OF EXPERIMENT DESIGN INCLUDING VOLUMES OF SOLID AND AQUEOUS REACTANTS—SERIES II-CAGB

	EXPT. 1	EXPT. 4	EXPT. 5
	SOLIDS		
Hornblende	0.0059 cm^3	0.0080 cm^3	0.0148 cm^3
Quartz	0.0069	0.0055	0.0035
Pyrite	0.0091	0.0084	0.0084
Microcline	0.0079	0.0103	0.0099
Magnetite	0.0042	0.0052	0.0039
Anhydrite	0.0032	0.0057	0.0052
Chalcopyrite	0.0111	0.0101	0.0132
Rutile	0.0094	0.0122	0.0084
	FLUIDS		
0.10 H_2SO_4 – K_2SO_4	0.601 cm^3	0.598 cm^3	0.597 cm^3
PRESSURE	1Kbar	1Kbar	1Kbar
TEMPERATURE	500°C	500°C	500°C
DURATION	18 days	18 days	18 days

TABLE 3. DETAILS OF EXPERIMENT DESIGN—SERIES III-CAGB

	EXPT. 1	EXPT. 2	EXPT. 4	EXPT. 5
FRESH HORNBLENDE VOLUME	0.0249 cm^3	0.0384 cm^3	0.0267 cm^3	0.0392 cm^3
RESULTING TEXTURE	Biotite rims + hornblende cores	Faint biotite rims + large hornblende cores	biotite rims + hornblende cores	Faint biotite rims + large hornblende cores

fluid/hornblende ratio, biotite forms complete rims around hornblende crystals and grows preferentially in cleavages or fractures in the hornblende. At higher values, biotite completely replaces hornblende, but generally preserves cleavage traces of the original grain.

The degree to which this biotitization reaction progressed varies as a function of temperature and fluid/hornblende ratio in the charge. Tables 1, 2 and 3 summarize textural observations from the experiments, along with data on the initial fluid/hornblende values. In the I-CAGB series of reactions (Table 1), complete biotitization occurred at 300 to 400°C, but fresh hornblende cores were preserved in the 500°C experiment, which contained a lower fluid/hornblende ratio. Series II-CAGB and III-CAGB (Tables 2, 3), all run at 500°C but with different values of the fluid/hornblende ratio, substantiated the relationship between this parameter and the extent of biotitization. This is illustrated in Figure 2, which shows the relative extent of biotitization as a function of fluid/hornblende ratio. In the products of experiments I-CAGB-4, II-CAGB-5 and III-CAGB-1 and -4, with values of the fluid/hornblende ratio between 119 and 54, the grains show an extensive rim of biotite while still containing a core of fresh hornblende. Experiments with "complete biotitization" all feature a fluid/hornblende ratio above 74. Those with only an incipient rim of biotite present (III-CAGB-3 and -5) have values of 13.38 and 13.24. It thus appears that a fluid/hornblende ratio between 54 and 74 represents the region in which the last primary hornblende is altered to biotite at the specific conditions of 500°C and 1 kilobar pressure.

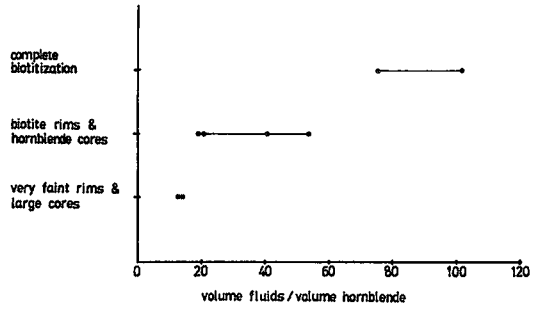

FIG. 2. Experimental results showing degree of biotitization as a function of fluid-to-hornblende volume ratio. T of experiments 500°C, P 1 kbar, fluid 0.1 m H_2SO_4 – K_2SO_4, mean grain-size 155 μm.

ELECTRON-MICROPROBE DATA OBTAINED ALONG GRAIN TRAVERSES

The varying degree of alteration makes it necessary to examine electron-microprobe data in terms of particular regions or zones within each hornblende grain. Rims, cores and some cleavages form areas that are discrete compositional units. A particularly good example of the various regions of alteration is observed in a grain from experiment II-CAGB-5 (Fig. 3). Five zones, labeled A, B, C, D and E, have been encountered in a microprobe traverse. Zones A and E are "biotite rims", B and D are "hornblende cores", and zone C is most likely a permeable region of cleavage or fracture. The traverse taken is represented by a solid line, with centres of "hornblende cores" analyzed at 10 μm intervals, whereas areas of compositional transition were analyzed in intervals of 2 μm. Average values for fresh hornblende (1) and zones A through E are listed in Table 4. There are significant differences between the

TABLE 4. ELECTRON-MICROPROBE RESULTS. ANALYSIS (1) IS STARTING HORNBLENDE, A THROUGH E ARE REACTION ZONES.

		II CAGB–5(e)				
	1	A (5 pts)	B (25 pts)	C (21 pts)	D (9 pts)	E (3 pts)
SiO_2	49.48	46.29	47.98	34.75	46.56	42.63
TiO_2	0.48	1.12	1.00	1.33	1.28	1.51
Al_2O_3	3.85	5.81	5.73	6.28	6.26	6.40
FeO	14.10	12.06	14.32	13.85	15.43	12.54
MgO	13.60	17.89	11.57	12.21	11.78	16.60
MnO	0.55	0.49	0.60	0.51	0.60	0.50
CaO	12.10	0.93	11.51	7.47	11.70	1.37
K_2O	0.34	6.30	1.01	7.32	1.05	6.31
Na_2O	0.72	0.07	1.09	0.04	1.15	0.02
F	0.32	0.29	0.28	0.22	0.25	0.26
Cl	0.04	0.01	0.02	0.00	0.03	0.00
SO_3	0.02	0.31	0.35	12.42	0.74	0.55
NiO	—	0.01	0.01	0.03	0.03	0.05
CuO	—	0.02	0.00	0.00	0.00	0.00
ZnO	—	0.00	0.00	0.01	0.00	0.00
BaO	—	0.02	0.01	0.01	0.01	0.01
TOTAL	95.60	93.62	95.48	96.45	96.87	90.75

$CaO/(CaO + SO_3)$ in zone C = .375 versus .419 for anhydrite.

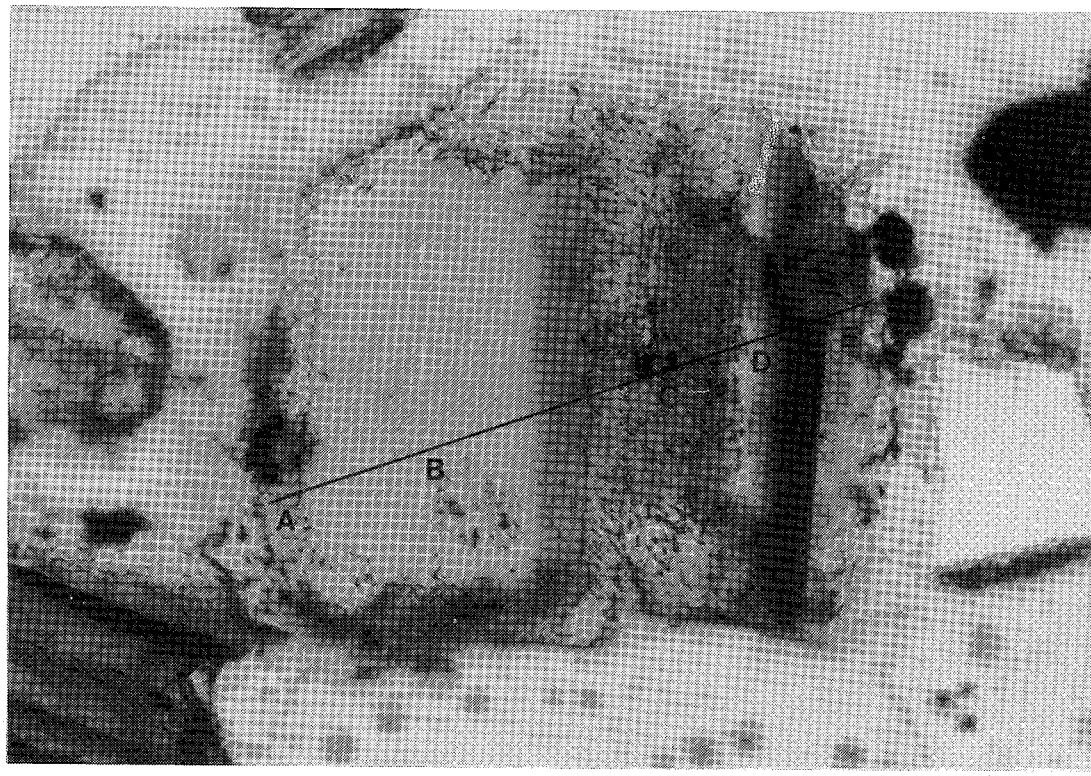

FIG. 3. Photomicrograph of experiment II–CAGB–5 showing biotite rim surrounding and penetrating hornblende core. Zones are labeled A (biotite rim), B (hornblende core), C (internal biotite replacement), D (hornblende core), and E (biotite rim).

altered "rim" regions and the altered region in zone C. Calcium and SO_3 are abundant in zone C, whereas "rims" are depleted in these components, with biotite again being the dominant phase. This relation is similar to that found in "completely biotitized" grains, where Ca and SO_3 concentrations are higher in the central regions, suggesting that biotite and anhydrite are two important secondary phases in the initial stages of alteration, and that as alteration progresses, Ca and SO_3 are mobilized, whereas biotite components remain fixed. Another possible explanation for high Ca values in areas such as altered "cores" or fractures could be that Ca^{2+} ions cannot diffuse with as much facility in central parts of a grain as they can near edges. It is possible that chemical-potential gradients are smaller in these regions, as the diffusion distance is greater.

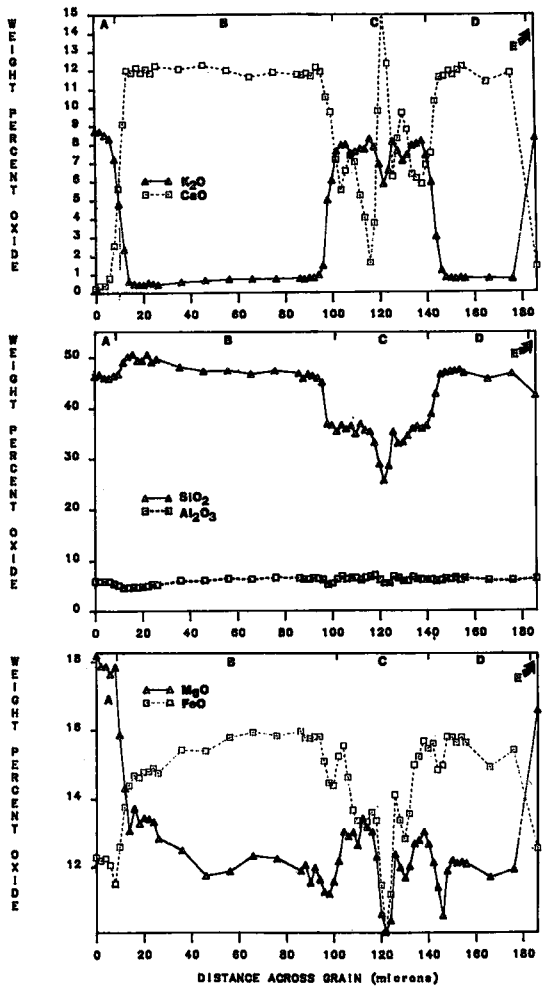

FIG. 4. Electron-microprobe data for K, Ca, Si, Al, Mg and Fe variation with distance across a traverse through zones A, B, C, D and E, as shown in Figure 3. Zone C contains sporadic anhydrite, resulting in the Ca variation shown. Elements are plotted as oxides.

Figure 4 (top) shows the antipathetic relation between K and Ca observed in the traverse shown in Figure 3, which is consistent in the "hornblende cores" (zones B and D) and "biotite rims" (zones A, C and E). Zone C, however, shows erratic variation in K and Ca and could represent biotite intermixed with a calcium-rich phase (anhydrite?) on a relatively fine scale. Silica, as expected, is depleted in altered zones (Fig. 4, middle), with the minimum SiO_2 concentration correlating with areas of abundant Ca and SO_3.

Consistently low Al_2O_3 values in secondary biotite point to a paucity of free Al^{3+} in the experimental system. Occupancy of octahedral and tetrahedral sites by aluminum in the newly formed biotite is comparable to aluminum site-occupancies in the fresh hornblende, and could thus be considered a remnant of the original, double-chain structure, as the experimental fluid contained no Al^{3+} at the start of the experiment. Si^{4+} dominates tetrahedral sites in biotitized rims, whereas Mg^{2+} fills the majority of octahedral positions as "FeO" is liberated (Fig. 4, bottom; Table 4) into the coexisting aqueous fluid.

X-Ray-Diffraction Studies and Structural Models for the Reaction Interface

Powder-diffraction patterns confirm the identity of the secondary biotite; in addition, a preliminary single-crystal study was performed in order to check for structural relationships between biotite and hornblende. Structural relations between crystals of biotite and hornblende can be determined from the Weissenberg and precession X-ray patterns taken. Figure 5 shows a first-octant stereographic projection of crystal-face orientation as encountered in the pseudomorphically replaced hornblende from experiment III–CAGB–4. Note that the (*h*00), (*hk*0) and the (0*k*0) of hornblende correspond to the (00*l*), (0*kl*) and (0*k*0) of biotite, but that other faces shown are mismatched by two to five degrees.

Veblen & Buseck (1980) have reported a comparable replacement-texture between coherent talc and anthophyllite. There, talc is intergrown with anthophyllite so that its y axis is parallel or subparallel to the anthophyllite y axis, and its z^* is parallel or nearly so to the anthophyllite x^*. Using a parallel argument, Figure 6A shows a portion of the hornblende–biotite interface represented on the scale of a TEM image. Noteworthy are the boundary areas along the hornblende (100) and (110), where transitions of double chains into infinite-width chains (*i.e.*, phyllosilicate structure) are accompanied by gaps that are predicted by the termination rules dis-

cussed by Veblen & Buseck (1980). These gaps, or three-dimensional tunnels, are parallel to the amphibole z axis and could be conduits for fast-diffusing ions during alteration. Using the model of Veblen & Buseck (1980), the (010) of hornblende containing no large tunnels would have only an ordinary rate of diffusion, and formation of biotite there would be slow in comparison with that along the (100) and (110) interfaces.

Figure 6B represents the region surrounding one hypothetical tunnel along the biotite–hornblende reaction interface (from circled "tunnel" in Fig. 6A). According to X-ray data and average values for unit-cell dimensions in amphiboles and micas (Deer *et al.* 1966), the width of the hornblende and biotite T-O-T layers is approximately 9.5 and 9.2 Å, respectively, giving a tunnel diameter in this configuration of about 4.5 Å. The $M(4)$ and A sites in hornblende, along with the interlayer K site of biotite, border directly on the tunnel and could be easily occupied or vacated during transport of ions along this conduit. In hornblende the A site is sometimes occupied by Na^+ and K^+, whereas $M(4)$ sites usually hold Ca^{2+} (Hawthorne 1983). From microprobe data described above, depletion of Na^+ and Ca^{2+} during biotitization of hornblende is strong, and therefore evacuation along these reaction-interface tunnels would seem a likely mechanism. Potassium enrichment can occur by occupation of the A site, which becomes equivalent to the interlayer K site in biotite, as double chains transform to infinite-width chains. Tunnel diameters can easily accommodate large cations such as K^+, Ca^{2+} and Na^+, with atomic radii of 1.33, 0.99 and 0.95 Å, respectively (Pauling 1960), so that significant transport of material is possible.

Microprecipitates of SiO_2 (Veblen & Ferry 1983) deposited in the interlayer planes of biotite could explain the complex chemical composition observed in certain altered grains. Alternatively, the presence of tunnels suggests another possible explanation. If cation diffusion along the hornblende (010) interface is much slower than in borders with tunnels, then removal of Ca^{2+} will also proceed more slowly. Therefore, likely areas for formation of calcium-rich phases such as anhydrite might be in planes parallel to the hornblende (010) or in zones directly adjacent to a (010) face of hornblende.

Representation of the Hornblende-to-Biotite Reaction In Terms of Solution Composition

The stoichiometry of the biotitization reaction described above and schematically represented as hornblende + K_2SO_4 + H_2SO_4 → biotite + quartz + anhydrite clearly depends on the composition of the hornblende and biotite involved. Because hornblende

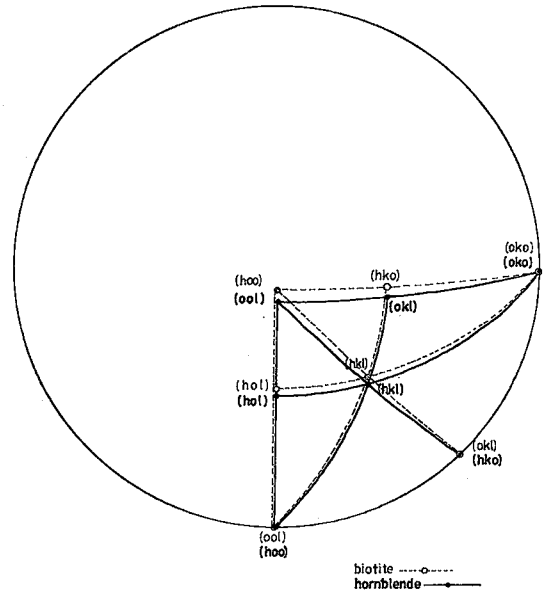

FIG. 5. Stereographic projection of the orientation of secondary biotite with respect to the host crystal of hornblende.

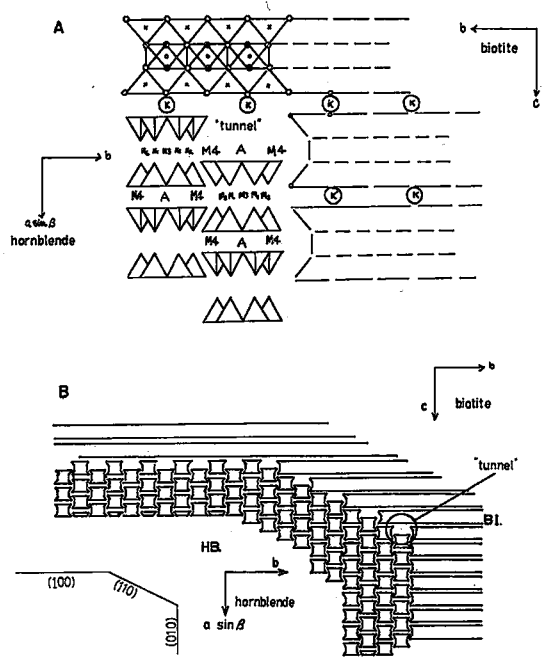

FIG. 6. A. Structural diagram of hornblende–biotite interface, showing position of proposed three-dimensional tubes in which large cations may be transported (after Veblen & Buseck 1980). B. Crystal structures of hornblende and biotite, illustrating the octahedral and tetrahedral sites.

in particular can show wide compositional variation, the real biotitization reaction will be equally variable. However, by a judicious choice of end-member components, this reaction, along with similar reactions that produce chlorite as an alteration product of hornblende or biotite, can be represented on a single activity-diagram that graphically illustrates the effect of the chemistry of the aqueous solution on mineral equilibria. By considering the composition of the natural starting materials, the most appropriate amphibole end-member can be selected for use on this activity diagram.

Fresh hornblende from the Butte deposit is generally intermediate between edenite and tremolite, a relatively low-aluminum hornblende. Edenite has therefore been selected as the hornblende component in the activity diagram shown in Figure 7, as appreciable K and Na are present (composition 1 in Table 4). In addition, stability fields of phlogopite and clinochlore are shown. These end members neglect the presence of ferric iron in the natural materials; however, it can be shown that the relative amounts of iron and magnesium in the solid phases do not affect the dependence of the reaction on the H_2SO_4 and K_2SO_4 activities, the variables of interest in the current study.

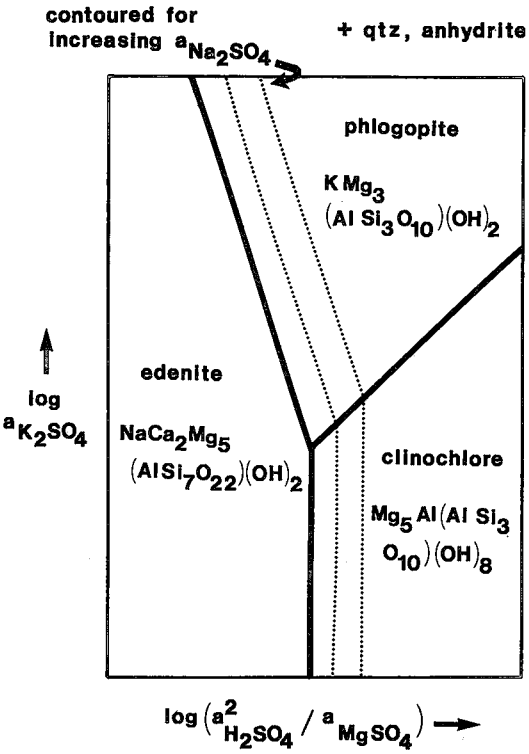

FIG. 7. Schematic activity-diagram showing relative stability-fields of edenite, phlogopite and clinochlore with respect to activities of aqueous species K_2SO_4, H_2SO_4, Na_2SO_4 and $MgSO_4$, in the presence of quartz and anhydrite. Dashed lines show the effect of increasing Na_2SO_4 activity.

The reactions upon which Figure 7 is based are written conserving aluminum in the solid phases and assuming the presence of quartz and anhydrite.

These reactions are:

$$\underset{\text{edenite}}{NaCa_2Mg_5(AlSi_7O_{22})(OH)_2} + \tfrac{1}{2}\underset{(aq)}{K_2SO_4} + 4\underset{(aq)}{H_2SO_4} = \underset{\text{phlogopite}}{KMg_3(AlSi_3O_{10})(OH)_2} + 4\underset{\text{quartz}}{SiO_2} + 2\underset{\text{anhydrite}}{CaSO_4} + \tfrac{1}{2}\underset{(aq)}{Na_2SO_4} + 2\underset{(aq)}{MgSO_4} + 4H_2O \quad (1)$$

$$2\underset{\text{edenite}}{NaCa_2Mg_5(AlSi_7O_{22})(OH)_2} + 10\underset{(aq)}{H_2SO_4} = \underset{\text{clinochlore}}{Mg_5Al(AlSi_3O_{10})(OH)_8} + 4\underset{\text{anhydrite}}{CaSO_4} + \underset{(aq)}{Na_2SO_4} + 11\underset{\text{quartz}}{SiO_2} + 5\underset{(aq)}{MgSO_4} + 8H_2O \quad (2)$$

$$\underset{\text{clinochlore}}{Mg_5Al(AlSi_3O_{10})(OH)_8} + \underset{(aq)}{K_2SO_4} + \underset{(aq)}{MgSO_4} + 3\underset{\text{quartz}}{SiO_2} = 2\underset{\text{phlogopite}}{KMg_3(AlSi_3O_{10})(OH)_2} + 2\underset{(aq)}{H_2SO_4} \quad (3)$$

Note that even in this simplified system, four aqueous components still must be considered in representing equilibrium relations between these three solids. In Figure 7, a two-dimensional graphical representation of these four variables has been made possible by combining H_2SO_4 and $MgSO_4$ on one axis and contouring with respect to Na_2SO_4 activity. Increasing Na_2SO_4 activity will enlarge the stability field of edenite relative to both phlogopite and clinochlore, as shown by the dotted lines in the figure. The figure also illustrates that phlogopite may be produced from edenite by increases in the activity of K_2SO_4 or of H_2SO_4 (or of both), a result that has also been demonstrated by the experiments described above. At lower activity of K_2SO_4, it is evident that clinochlore would be the expected product of replacement of the amphibole. Numerical values have not been included in the figure owing to large uncertainties in the thermodynamic data for the aqueous species and the solid edenite at the temperatures of the experiments.

It is interesting to note that coefficients for the aqueous species in these reactions are dependent on the amount of aluminum in the amphibole. An increase in this aluminum content reduces the amount of H_2SO_4 involved in the reaction, and in highly aluminous amphiboles, H_2SO_4 and $MgSO_4$ actually switch sides in the reaction, as in the case of the amphibole pargasite, which may form phlogopite in the following reaction:

$$\underset{\text{pargasite}}{NaCa_2Mg_4Al(Al_2Si_6O_{22})(OH)_2} + 5\underset{(aq)}{MgSO_4} +$$
$$\tfrac{3}{2}\underset{(aq)}{K_2SO_4} + 3\underset{\text{quartz}}{SiO_2} + 6H_2O =$$
$$3\underset{\text{phlogopite}}{KMg_3(AlSi_3O_{10})(OH)_2} + 2\underset{\text{anhydrite}}{CaSO_4} +$$
$$4\underset{(aq)}{H_2SO_4} + \tfrac{1}{2}\underset{(aq)}{Na_2SO_4} \qquad (4)$$

However, for many common igneous amphiboles, reaction (1) is more appropriate, and this is certainly the case in the experiments discussed above.

Reactions similar to (1) and (4), but written with chloride instead of sulfate aqueous species, are presented by Eastoe (1982) in a discussion of the hornblende-to-biotite reaction inferred in the Panguna porphyry copper deposit.

Mineralogical Path of Reaction and Comparison with Natural Systems

In porphyry-copper deposits, hydrothermal biotite is typically more magnesian than igneous biotite (Roberts 1973) and contains less Ti (Brimhall 1977). An overall test of the applicability of our experimental results, then, is to check our data against these ubiquitous effects. Paths of hydrothermal reactions in natural biotite compositions have been studied (Munoz & Swenson 1981, Gilzean & Brimhall 1984, Brimhall *et al.* 1983). In Figure 8 we present a composite diagram showing biotite compositions in terms of log (X_F/X_{OH}) *versus* log (X_{Mg}/X_{Fe}) octahedral. In the lower right corner we show the position of products from hydrothermal experiments. The averaged compositions of rim biotite surrounding a hornblende core are shown as hexagons (experiments II-CAGB-5 average). The com-

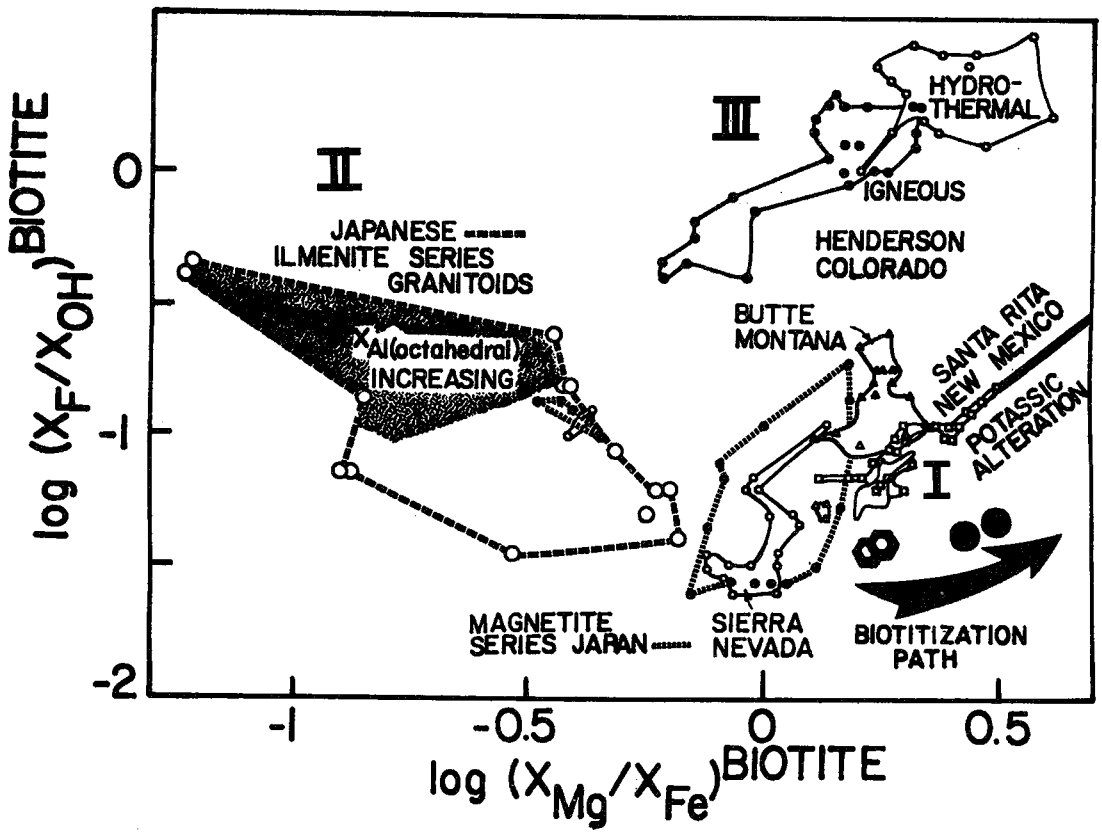

FIG. 8. Plot of biotite compositions showing path of hydrothermal reaction in our experiments in relation to path of potassic alteration at Santa Rita, New Mexico. Three types of intrusive system are also shown: I) I-type granites related to porphyry-copper deposits, II) S- or I-type granites of the ilmenite series of Japan, related in some cases to tin-tungsten deposits, and III) anorogenic Mo-rich systems *(e.g.,* Henderson, Colorado).

positions of biotite in completely biotitized grains with no hornblende core are shown as solid circles (experiments II-CAGB-1 and -4). These completely biotitized grains are more phlogopitic than the rim biotite and have a slightly higher log X_F/X_{OH}. The path of hydrothermal reaction is shown by a solid black arrow. In the same systems of co-ordinates (Fig. 8) we show compositions of natural biotite from three distinct types of igneous system. Type I indicates the field of biotite from I-type intrusive bodies, *e.g.*, the Sierra Nevada suite (Dodge *et al.* 1969), the Boulder batholith of Montana (Brimhall *et al.* 1983), the magnetite series of Japan (Czamanske *et al.* 1981), and the Santa Rita porphyry copper deposit (Jacobs 1976, Jacobs & Parry 1979). The compositions of hydrothermal biotite, part of the potassium silicate alteration assemblage at Santa Rita, New Mexico, forms a linear array with a positive slope representing an isotherm (Munoz & Swenson 1981) for a process of high-temperature alteration. Our experimental data-points show that at 500°C, the direction and slope of reaction are toward higher values of the Mg/Fe ratio in the biotite, in accord with natural exchange-isotherms. Our experimental results appear, therefore, to reflect the natural paths of reaction of the biotitization of hornblende at Santa Rita. We show in Figure 8 two other magmatic–hydrothermal systems in terms of biotite compositions. Type II represents typical S- or mixed S- and I-type granites, *e.g.*, the ilmenite series of Japan (Czamanske *et al.* 1981). Type III are anorogenic intrusive bodies, *e.g.*, the Henderson deposit in Colorado (Gunow *et al.* 1980). The ore deposits for types I, II and III are copper, tin–tungsten and molybdenum, respectively (Munoz & Swenson 1981, Gilzean & Brimhall 1983).

Conclusions

Hydrothermal experiments have produced the biotitization of hornblende at temperatures of 300 to 500°C at 1 kilobar. The main factors controlling the completeness of the reaction are time and the volume ratio of fluid to hornblende for a certain range in size of starting hornblende crystals. Biotitization reactions in K_2SO_4–H_2SO_4–H_2O fluids produce biotite compositions very near those of the natural hydrothermal phase. Mineralogical reaction-paths in terms of increasing X_F/X_{OH} and X_{Mg}/X_{Fe} are also similar to paths in biotite from porphyry-copper deposits.

The net chemical effect of the pseudomorphic replacement of hornblende by biotite is to fix Mg^{2+}, SO_4^{2-}, and K^+ in the mineral assemblage as a mixture of biotite and anhydrite. The aqueous fluid, in contrast, becomes enriched in Fe^{2+} and Ca^{2+}. Silica, released by the destruction of hornblende, probably precipitates as quartz, and the iron as pyrite plus chalcopyrite, implying a link with the mineralizing process.

Single-crystal-diffraction studies indicate a nearly perfect alignment of the hydrothermal biotite with the crystal structure of the original hornblende. Three-dimensional tubes are inferred to occur between the structure of both minerals, parallel to the *C* axis of the hornblende. These tubes may represent avenues for cation transport from the coexisting fluid.

Acknowledgements

The impetus for this study was the field work of the late Steven Roberts, friend and colleague of the senior author for years. His insight, enthusiasm and wit have been sorely missed. NSF grant EAR-8115907 has supported this study. Some of the electron-microprobe analyses were performed by David Sassani. Thoughtful reviews by R.F. Martin and G.M. Anderson improved the manuscript significantly. Their comments are appreciated. We also thank Adolf Pabst for his preliminary X-ray-diffraction studies.

References

Brimhall, G.H., Jr. (1977): Early fracture-controlled disseminated mineralization at Butte, Montana. *Econ. Geol.* **72**, 37-59.

_____ (1979): Lithologic determination of mass transfer mechanisms of multiple-stage porphyry copper mineralization at Butte, Montana: vein formation by hypogene leaching and enrichment of potassium-silicate protore. *Econ. Geol.* **74**, 556-589.

_____ (1980): Deep hypogene oxidation of porphyry copper potassium-silicate protore at Butte, Montana: a theoretical evaluation of the copper remobilization hypothesis. *Econ. Geol.* **75**, 384-409.

_____, Cunningham, A.B. & Stoffregen, R. (1984): Zoning in precious metal distribution within base metal sulfides: a new lithologic approach using generalized inverse methods. *Econ. Geol.* **79**, 209-226.

_____ & Ghiorso, M.S. (1983): Origin and ore-forming consequences of the advanced argillic alteration process in hypogene environments by magmatic gas contamination of meteoric fluids. *Econ. Geol.* **78**, 73-90.

_____, Gilzean, M. & Burnham, C.W. (1983): Magmatic source region, protoliths and controls on metallogenesis: mica halogen geochemistry. *Amer. Geophys. Union Trans.* **64**, 884 (abstr.)

CZAMANSKE, G.K., ISHIHARA, S. & ATKIN, S.A. (1981): Chemistry of rock-forming minerals of the Cretaceous–Paleocene batholith in southwestern Japan and implications for magma genesis. *J. Geophys. Res.* **86,** 10431-10469.

DEER, W.A., HOWIE, R.A. & ZUSSMAN, J. (1966): *An Introduction to the Rock-Forming Minerals.* Longman, London.

DODGE F.C.W., SMITH, V.C. & MAYS, R.E. (1969): Biotites from granitic rocks of the central Sierra Nevada Batholith, California. *J. Petrology* **10,** 250-271.

EASTOE, C.J. (1982): Physics and chemistry of the hydrothermal system at the Panguna porphyry copper deposit, Bougainville, Papua New Guinea. *Econ. Geol.* **77,** 127-154.

GILZEAN, M.N. & BRIMHALL, G.H. (1983): Alteration biotite chemistry and nature of deep hydrothermal system beneath Silverton District, Colorado. *Geol. Soc. Amer. Abstr. Programs* **15,** 581.

GUNOW, A.J., LUDINGTON, S. & MUNOZ, J.L. (1980): Fluorine in micas from the Henderson molybdenite deposit, Colorado. *Econ. Geol.* **75,** 1127-1137.

HAWTHORNE, F.C. (1983): The crystal chemistry of the amphiboles. *Can. Mineral.* **21,** 173-480.

JACOBS, D.C. (1976): *Geochemistry of Biotite in the Santa Rita and Hanover–Fierro Stocks, Central Mining District, Grant County, New Mexico.* Ph.D. thesis, Univ. Utah, Salt Lake City, Utah.

_____ & PARRY, W.T. (1979): Geochemistry of biotite in the Santa Rita porphyry copper deposit, New Mexico. *Econ. Geol.* **74,** 860-887.

MOORE, W.J. & CZAMANSKE, G.K. (1973): Compositions of biotites from unaltered and altered monzonite rocks in the Bingham Mining District, Utah. *Econ. Geol.* **68,** 269-274.

MUNOZ, J.L. & SWENSON, A. (1981): Chloride-hydroxyl exchange in biotite and estimation of relative HCl/HF activities in hydrothermal fluids. *Econ. Geol.* **76,** 2212-2221.

PAULING, L. (1960): *The Nature of the Chemical Bond (3rd ed.).* Cornell University Press, Ithaca, N.Y.

ROBERTS, S.A. (1973): Pervasive early alteration in the Butte District, Montana. *Soc. Econ. Geol. Guidebook, Butte Field Mtg.* **HH1-HH8.**

TITLEY, S.R. (1982): Mineralization and alteration in porphyry copper systems. *In* Advances in Geology of the Porphyry Copper Deposits in Southwestern North America (S.R. Titley, ed.). University of Arizona Press, Tucson, Arizona.

VEBLEN, D.R. & BUSECK, P.R. (1980): Microstructures and reaction mechanisms in biopyriboles. *Amer. Mineral.* **65,** 599-623.

_____ & FERRY, J.M. (1983): A TEM study of the biotite–chlorite reaction and comparison with petrologic observations. *Amer. Mineral.* **68,** 1160-1168.

Received May 15, 1984, revised manuscript accepted February 13, 1985.